Journal of the European Ceramic Society 19 (1999) 759–763

PII: S0955-2219(98)00307-0
0955-2219/99/$ - see front matter

High-load Resistors of Doped Titanate Ceramics Showing PTCR Behavior in the Entire Temperature Range of Operation

Ralf Moos,* Marco Fandel and Wolfgang Schäfer

Dornier GmbH, Daimler-Chryster Research Center, 88039 Friedrichshafen, Germany

Abstract

Ceramic high-load resistors of donor-doped strontium titanate were manufactured and successfully tested. The samples do not only withstand short high-load pulses (10 ms) with a power loss of ~1MW, but also show a PTCR behavior in the entire temperature range of operation. Compared to the common $BaTiO_3$-PTCR devices, the samples do not exhibit a grain-boundary controlled resistance, that results in thermo-mechanical stress-induced failure of the devices. The PTCR behavior is a bulk effect, originating from the temperature dependent mobility, that obeys a strong power law. The comparison between thermopower and resistivity measurements has proven to be an excellent method to distinguish between grain boundary-controlled and bulk-controlled resistivity. © *1999 Elsevier Science Limited. All rights reserved*

Keywords: titanates, electrical conductivity, thermal shock resistance, perovskites, thermistors.

1 Introduction

At present, high-load resistors are mostly made of metallic alloys. In order to obtain devices with a well-defined resistance, the devices are manufactured of thin coiled wires. Typical values for the resistivity ρ of the materials that are used are between $0{\cdot}5\times10^{-6}\,\Omega$m for constantan and $1\times10^{-6}\,\Omega$m for NiCr alloys. Thicker and therefore longer wires are required, if the resistors are to be used for high-current applications. Then, the inductance of these coiled devices cannot be neglected anymore. However, high currents often have to be switched by solid-state or conventional relays. In order to avoid spikes of high voltages and to achieve a fast current rise time, the inductance should be as low as possible. This means that most high-load resistor applications demand disc-shaped geometries and therefore materials with relatively high resistivities ρ. Moreover, a positive temperature coefficient of resistivity (PTCR) is absolutely required since, otherwise, it is not possible to obtain a stable operation mode.

Ceramic PTCR-devices are well known. Usually, they are manufactured of titanates and show a temperature coefficient of resistance, α, up to $+100\%$K around the Curie temperature, T_C, where the lattice switches from the tetragonal to the cubic state. However, α becomes negative a few degrees below and above T_C. A recent review gives a comprehensive summary[1] of the research that has been conducted since the seventies, when the groups of Heywang[2] and Härdtl[3] found out that the PTCR effect was caused by acceptor states being located at the grain boundaries of the donor-doped barium titanate based ceramics. However, for high-load applications these PTCR ceramics have the disadvantage that almost the complete power loss occurs at the -compared to the bulk- high ohmic grain boundaries. This leads to a strong inhomogeneous distribution of heat that may destroy the ceramic device, especially if the current is switched in pulses. Another limitation is the non-monotonous R–T-characteristic and the extreme change in resistance by several decades that cannot be accepted for some special applications.

In order to obtain low-volumed (a few cm^3) disc-shaped electric resistor devices with low inductance, showing a PTCR behavior in the entire temperature range, and being suitable to withstand short high-current pulses (10 ms, power loss ~1MW), a new ceramic approach has been conducted taking advantage of the strong temperature dependence of the mobility of the electronic charge carriers in donor-doped titanate ceramics. The desired resistance of the device in addition to the

*To whom correspondence should be addressed. Fax: +49-7545-8-14265; e-mail: ralf.moos@daimlerchrysler.com

geometric boundary conditions (diameter and thickness) determines the resistivity of the materials to be used. Since high-ohmic grain boundaries and high-ohmic electrode contact resistance cannot be accepted due to the reasons mentioned above, two degrees of freedom remain to design the ceramic resistivity: the charge carrier density n and their carrier mobility μ

$$\rho = (e \times n \times \mu)^{-1} \tag{1}$$

Both n and μ can be calculated in advance by defect chemical considerations.

2 Short Overview on Transport Properties and Defect Chemistry of Titanates

The electronic mobility, μ, of donor (lanthanum) doped strontium titanate, $Sr_{1-x}La_xTiO_3$, obeys a strong power law

$$\mu(T) \propto T^{-M} \tag{2}$$

with $M = 2.7$ at room temperature for undoped[4–6] and slightly doped samples.[7,8] Lanthanum is an ideal donor in $SrTiO_3$, that is ionized even at 4·2 K.[9] The solubility of the donor lanthanum in $SrTiO_3$ is neither limited in reducing nor in oxidizing atmospheres.[10,11] However, the reducing power of the high-temperature processing atmospheres during calcining and sintering has to be exactly controlled since, otherwise, the charge carrier densities and the concentration of added lanthanum donors, [La], will not be equal.

$$n = [\mathrm{La}] \tag{3}$$

A very strong reducing atmosphere leads to the formation of donor-type oxygen vacancies and to an increase in electronic charge carriers, whereas under poor reducing or oxidizing conditions, the ceramics form shear structures by incorporating donor type excess oxygen and by forming strontium vacancies. The samples become insulators. A very comprehensive survey of the defect chemistry of $SrTiO_3$ allowing the calculation of high-temperature processing conditions as well as the transport properties of these ceramics can be found in Ref. 12.

Figure 1 illustrates this behavior for typical sintering temperatures. At low oxygen partial pressures (i.e. strongly reducing atmospheres), both oxygen vacancy concentration and carrier density decrease with oxygen partial pressure (slope of $-1/6$ in the log–log plot) until the oxygen vacancy concentration becomes negligible compared to the lanthanum donor content. A further increase in

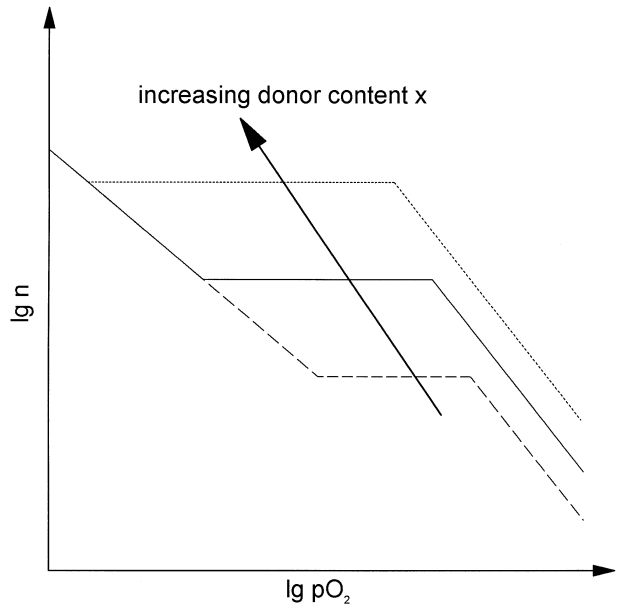

Fig. 1. Defect chemistry of $SrTiO_3$: schematic log–log plot of the charge carrier density, n, at sintering temperature versus oxygen partial pressure, pO_2, of the sintering atmosphere. Parameter: lanthanum donor content x.

pO_2 does not affect the carrier density anymore and, in accordance to eqn (3), the charge carrier density only depends on the lanthanum donor concentration. Therefore this range is also called 'plateau region'. A further increasing pO_2 of the sintering atmosphere leads to insulating ceramics due to the compensation of donors by acceptor type excess oxygen.[12] Due to the thermodynamic character of the defect chemistry, it becomes obvious that these distinct pO_2-ranges also depend on temperature. For the preparation of ceramic resistor devices, the samples should be sintered under conditions concerning pO_2 and T that meet the requirements for the plateau region, leading to

$$\rho = (e \times [\mathrm{La}] \times \mu)^{-1} \tag{4}$$

In conjunction with the mobility values obtained in several other studies,[4–7] the temperature-dependent resistivity $\rho(T)$ can be calculated. Equation (4) is plotted in Fig. 2(a) for different donor contents. The highest values for the resistivity can be obtained for a lanthanum content of $[\mathrm{La}] = 5{\cdot}1 \times 1 \times 10^{18}$ $\mathrm{cm}^{-3}(x = 0{\cdot}0003)$. A donor content below that value leads to insulating ceramics due to the intrinsic acceptor concentration that compensates the lanthanum donors.[12] Above $x = 0{\cdot}3$, the samples become degenerated semiconductors[11] and the charge carrier transport mechanism changes from phonon scattering to an impurity-controlled behavior. Then the power law of the temperature dependence is not anymore valid.[8] Fig. 2(b) shows the temperature coefficient α calculated from Fig. 2(a) using eqn (5)

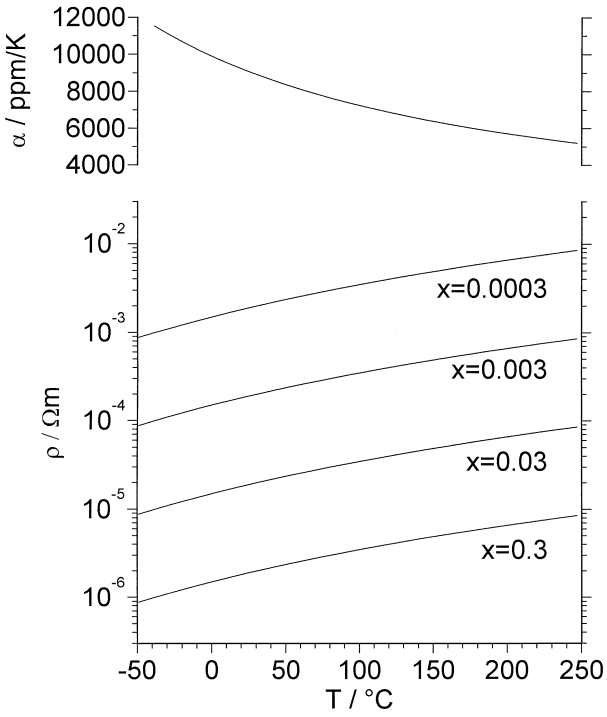

Fig. 2. (a): resistivity, ρ, of donor-doped strontium titanate versus temperature as calculated from eqn (1) and eqn (4). Parameter lanthanum donor content x in $Sr_{1-x}La_xTiO_3$. (b): Temperature coefficient of resistivity, α, calculated with eqn (5) from the curves in the lower figure. Note: α does not depend on the donor content.

$$\alpha = \frac{1}{\rho(T)} \times \frac{\mathrm{d}\rho(T)}{\mathrm{d}T} \tag{5}$$

As can be seen, α reaches values $>10\,000$ ppm/K and α does not depend on the absolute value of the resistivity since it depends only on the temperature dependence of the mobility which is independent on the lanthanum concentration.[8]

3 Experiment

3.1 Preparation

Lanthanum-doped strontium titanate powders were prepared by a conventional mixed-oxide technique starting from $SrCO_3$, TiO_2 and La_2O_3. In order to improve sinterability, 1% (by mole) titania was added in excess. The $Sr_{1-x}La_xTi_{1.01}O_3$-powders were calcined at 1150°C and ground in a ball mill down to a particle size of about 2 μm (d_{50}). The XRD-analysis did not show any second phases except for traces of rutile. The samples were formed to disc-shaped pellets, isostatically pressed, and sintered in different reducing atmospheres at temperatures between 1350 and 1500°C to samples of about 25 g with a diameter of 35 mm and a thickness of 6 mm. In order to ensure the conditions of the 'plateau region', sintering was conducted in a water-saturated hydrogen/noble gas atmosphere. Saturation temperature and hydrogen content of the atmosphere were calculated using material constants of strontium titanate published in Ref. 12.

3.2 Electrical characterization

The resistivity of the pellets was determined in a simple sample holder between 10 and 90°C using a four-probe technique as described, for example, in Ref. 13 and an appropriate geometrical correction factor that was experimentally evaluated. In order to eliminate errors by thermoelectric effects, the measurements were conducted using a reversed-dc setup. The thermopower at room temperature of the same samples was determined in a set-up that has been described in Ref. 11. Electrodes were applied to the pellets using different metallization methods. The resistance of the metallized devices was measured and compared with the resistance values that were calculated from the four-probe experiments. The high load behavior of the devices was tested at room temperature using sinusoidal semioscillation pulses of about 10 ms. The voltage between the two electrodes of the devices was recorded with a data logger as well as the voltage drop of a serial resistor that indicated the current through the device.

4 Results and Discussion

Thermopower measurements offer a good chance to determine the charge carrier density of arbitrarily shaped samples without using a complex Hall effect test set-up. For the thermopower of a broad-band semiconductor, η, eqn (6) is valid:[11]

$$\eta = -\frac{k}{e} \times \left(\ln \frac{N_C(T)}{n} + A_e \right) \tag{6}$$

The effective density of states, N_C, is $2{\cdot}2 \times 10^{20}$ cm^3 at room temperature and the transport factor $A_e = 3$.[11] In Fig. 3, log ρ of each sample is plotted versus η. The sign of the temperature coefficient of the resistivity is marked by the symbols: the 'o'-symbol indicates $\alpha > 0$ and '•' stands for a negative temperature coefficient. The continuous line in Fig. 3 denotes the theoretical function which can easily be calculated by inserting eqn (1) in eqn (6) and by using a mobility of $\mu = 6$ cm^2 Vs at room temperature. This line is also the boundary between region I and region II. NTC behavior can be observed only in region III, above a line (dotted) that corresponds to five times the theoretical value.

This behavior fits very well with literature. Gerthsen *et al.*[14] showed that the influence of thin low-conducting grain boundaries on the thermopower

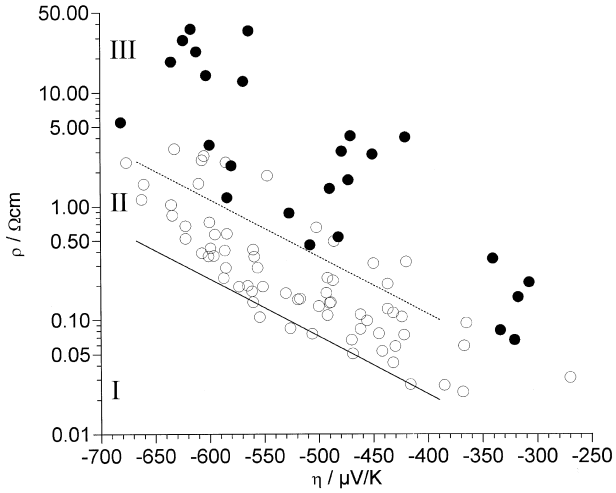

Fig. 3. Resistivity, ρ, of all tested samples versus thermopower, η. Data taken at room temperature. The 'o'-symbol indicates PTCR behavior, '•' indicates NTCR behavior. The continuous line represents the lower theoretical limit; the dotted line illustrates a resistivity that equals 5 times the theoretical values. For the meaning of the regions I,II, and III, refer to the text.

can be neglected. Therefore, the thermopower represents the charge carrier density of the bulk of a ceramic sample. If the influence of high-ohmic grain boundaries on the resistivity can be neglected, resistivity and thermopower data should meet eqn (6), represented by the continuous line. Therefore no symbols can be found in region I. The more the resistivities of the samples become grain boundary controlled, the more the distance between theoretical line and measured value increases and a negative temperature coefficient can be observed, because the barrier-like grain boundaries can be overcome by a thermally activated process.[8] This can be observed for the samples in region III, above the dotted line. Obviously, high-ohmic grain boundaries completely affect the conductivity in region III and the influence of the bulk behavior on the conductivity becomes negligible. Such samples do not meet the above-mentioned requirements for high-load resistor applications.

High-load pulse tests were performed with samples of region II, having thermopower values below $-600\,\mu$V/K. For these experiments, electrodes were applied and the resistance, R_{2pt}, of the devices was measured by a common two-probe technique. R_{2pt} was compared with the resistance R_{4pt} that was calculated from the four-probe measurements and the geometry data. The difference $R_{2pt} - R_{4pt}$ was assumed to be the contact resistance. For the high-current pulse tests, only those samples were chosen that had a negligible contact resistance.

Figure 4 shows the result of a successful high-current experiment of a 'o'-marked sample, with negligible contact resistance. At room temperature, the resistance of the sample (size see above) was

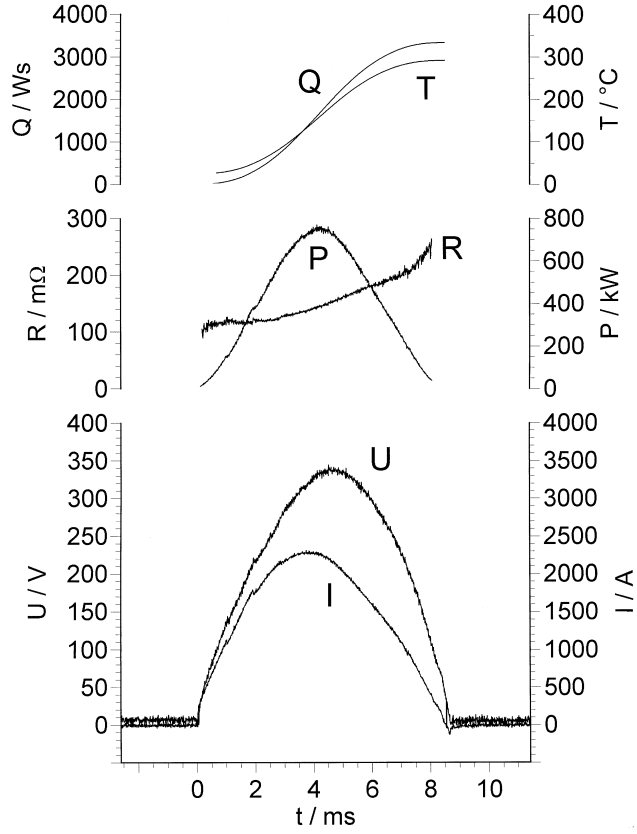

Fig. 4. Typical high-load pulse test. Bottom: voltage, U, and resulting current, I, as a function of time. Center: resistance, R, and power loss, P, both calculated from U and I. Top: accumulated dissipated energy, Q, and temperature, T, calculated from eqn (7).

120 mΩ. During the experiment the voltage, U, increased up to a peak value of 350 V. The current, I, reached a peak value of 2300A (bottom), and the power loss, $P = U \times I$, increased up to almost 800 kW. The resistance, $R = U/I$, is also plotted as well as the dissipated energy, Q, calculated from $Q = \int \mathrm{Pdt}$. A rough estimation of the temperature T can be calculated from eqn (7)

$$Q = c \times m \times (T - T_R) \tag{7}$$

In eqn (7), c denotes the heat capacity, m the mass of the samples, and T_R the room temperature.

Due to the increasing temperature and the PTCR-behavior of the device, it can be clearly seen that the resistance increases monotonously as a result of the high power loss. The current reaches its maximum before the voltage maximum and, because of the PTCR-behavior, the current is limited to 2300A instead of 2915A (= 350 V/120 mΩ). After an appropriate cooling time, the resistance reached its initial value of 120 mΩ. This experiment has been repeated several times without destroying the device. Several experiments with contact resistance-free 'o'-marked samples have been successfully conducted. However, '•'-marked NTC-type resistors always failed. The samples cracked mostly

in the middle of the device. The broken fragments were molten on the surface. For the sake of completeness, very few samples from region II but with non-negligible contact resistance values had been also tested. All these devices were destroyed at the metallization.

5 Conclusion

Ceramic high-load resistors of donor-doped strontium titanate were manufactured and successfully tested. The samples do not only withstand short high-load pulses of 10 ms but also show a strong PTCR-behavior in the entire temperature range of operation.

References

1. Huybrechts, B., Ishizaki, K. and Takata, M., Review: The positive temperature coefficient of resistivity in barium titanate. *J. Mat. Sci.*, 1995, **30**, 2463–2474.
2. Heywang, W., Resistivity anomaly in doped barium titanate. *J. Am. Cer. Soc.*, 1964, **47**(10), 484–489.
3. Daniels, J., Härdtl, K. H. and Wernicke, R., The PTC effect of barium titanate. *Phil. Tech. Rev.*, 1978, **38**, 73–82.
4. Tufte, O. N. and Chapman, P. W., Electron mobility in semiconducting strontium titanate. *Phys. Rev.*, 1967, **155**, 796–802.
5. Lee, C., Destry, J. and Brebner, L. J., Optical absorption and transport in semiconducting $SrTiO_3$. *Phys. Rev. B*, 1975, **11**(6), 2299–2310.
6. Moos, R., Menesklou, W. and Härdtl, K. H., Hall mobility of undoped n type conducting strontium titanate single crystals between 19 K and 1373 K. *Appl. Phys. A.*, 1995, **61**, 389–395..
7. Uematsu, K., Sakurai, O., Mizutani, N. and Kato, M., Electrical properties of La-doped $SrTiO_3$ (0·1–2·0%) single crystals grown by xenon-arc image floating zone method. *J. Mat. Sci.*, 1984, **19**, 3671–3679.
8. Moos, R. and Härdtl, K. H., Electronic transport properties of $Sr_{1-x}La_xTiO_3$ ceramics. *J. Appl. Phys.*, 1996, **80**(1), 393–400.
9. Perluzzo, G. and Destry, J., The characterization of pure and niobium-doped crystals of strontium titanate using Hall, electrical conductivity, and optical absorption data. *Can. J. Phys.*, 1977, **56**, 453–467.
10. Moos, R., Bischoff, T., Menesklou, W. and Härdtl, K. H., Solubility of lanthanum in strontium titanate in oxygen-rich atmospheres. *J. Mat. Sci.*, 1997, **32**(16), 4247–4252.
11. Moos, R., Gnudi, A. and Härdtl, K. H., Thermopower of $Sr_{1-x}La_xTiO_3$ ceramics. *J. Appl. Phys.*, 1995, **78**(8), 5042–5047.
12. Moos, R. and Härdtl, K. H., Defect chemistry of donor doped and undoped strontium titanate ceramics between 1000°C and 1400°C. *J. Am. Cer. Soc.*, 1997, **80**(10), 2549–2562.
13. Smits F. M. Measurement of the sheet resitivities with the four-point probe. *Bell System Techn. J.*, 1958, 711–718.
14. Gerthsen, P., Härdtl, K. H. and Csillag, A., Mobility determinations from weight measurements in solid solutions of $(Ba,Sr)TiO_3$. *Phys. Stat. Sol. (a)*, 1972, **13**, 127–133.